SIMULATION OF HYDROGEN MIXING AND PAR OPERATION DURING ACCIDENTAL RELEASE IN AN LH2 CARRIER ENGINE ROOM

Kelm, S.[1], Baggemann, J.[1], Reinecke, E.-A.[1,*], Verfondern, K.[1], and Kamiya, S.[2]

[1] Institute of Energy and Climate Research (IEK-6), Forschungszentrum Juelich GmbH, 52425 Juelich, Germany, s.kelm@fz-juelich.de
[2] Kawasaki Heavy Industries, 1-1, Kawasaki-cho, Akashi City, 673-8666 Japan, kamiya_s@khi.co.jp
*** corresponding author: e.reinecke@fz-juelich.de**

ABSTRACT

Next-generation LH2 carriers may use the boil-off gas from the cargo tanks as additional fuel for the engine. As a consequence, hydrogen pipes will enter the room of the ship's propulsion system and transport hydrogen to the main engine. The hydrogen distribution resulting from a postulated hydrogen leak inside the room of the propulsion system has been analyzed by means of Computational Fluid Dynamics (CFD). In a subsequent step, simulations with passive auto-catalytic recombiners (PARs) were carried out in order to investigate if the recombiners can increase the safety margins during such accident scenarios. CFD enables a 3D prediction of the transient distribution with a high resolution, allowing to identify local accumulation of hydrogen and consequently to identify optimal PAR positions as well as to demonstrate the efficiency of the PARs. The simulation of the unmitigated reference case reveals a strong natural circulation, driven by the density difference of hydrogen and the incoming cold air from the ventilation system. Globally, this natural circulation dilutes the hydrogen and removes a considerable amount from the room of the ship's propulsion system via the ventilation ducts. However, a hydrogen accumulation beyond the flammability limit is identified below the first ceiling above the leak position and the back-side wall of the engine room. Based on these findings, suitable positions for recombiners were identified. The design objectives of the PAR system were on the one hand to provide both high instantaneous and integral removal rate and on the other hand to limit build-up of flammable clouds by means of depletion and PAR induced mixing processes. The simulations performed with three different PAR arrangements (variation of large and small PAR units at different positions) confirm that the PARs reduce efficiently the hydrogen accumulations.

1 INTRODUCTION

Kawasaki Heavy Industries (KHI) plans to build a large LH2 carrier to import LH2 from Australia in the future, and is currently building a small (pilot) LH2 carrier [1] for verifying the CO_2-free hydrogen energy supply chain [2] between Japan and Australia. The large LH2 carrier will use boil off gas as additional fuel as existing LNG carriers. In this case, two hydrogen feed lines will enter the engine room and transport hydrogen to the main boilers.

The accident scenario under consideration involves a power blackout, i.e., failure of the active ventilation system of the engine room. Furthermore, it is assumed that there is hydrogen leaking from one or both lines, which initially remains undetected. In this time, hydrogen may accumulate and form a locally flammable gas mixture with air. To prevent endangering the crew and the ship, several countermeasures are under discussion. The option investigated in this paper is the installation of passive auto-catalytic recombiners (PARs) which are established elements of the safety concept in nuclear power plants. PARs convert hydrogen into water vapor by means of passive mechanisms and have been qualified for operation under the conditions of nuclear power plant accidents [3]. The

working principle of a PAR is illustrated in Fig. 1. Inside the catalyst section, catalyst sheets form a set of parallel vertical flow channels. On the catalyst surface, hydrogen entering the PAR is converted with oxygen to water vapor. Due to the exothermal reaction, a buoyancy-driven flow is induced inside the chimney on top of the catalyst section. The chimney ensures an upward directed gaseous flow through the PAR which inherently feeds the surrounding hydrogen/air mixture into the catalyst section. Being an entirely passive safety measure, PARs will operate even in case of blackout and without crew interaction.

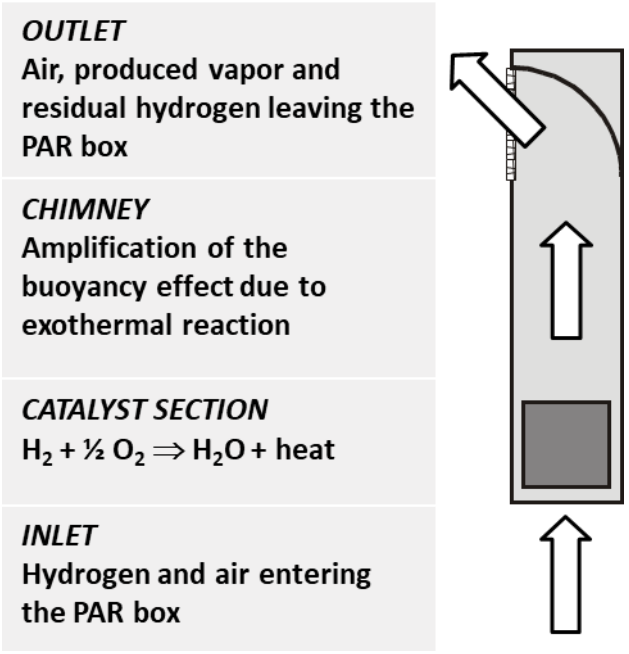

Figure 1. Working principle of a PAR

To cover a wide range of potential releases, hydrogen release rates of ~0.5g/s (break in one line) up to 4 g/s (break or failure of several lines) are analyzed. Furthermore, two generic recombiner designs based on existing recombiners from nuclear power plants [4] are considered for hydrogen mitigation. The simulations of hydrogen mixing and mitigation are performed using the commercial CFD package ANSYS CFX 15.0 [5] coupled with the in-house code REKO DIREKT [6,7].

Following the description of the modeling approach (chapter 2), the hydrogen distributions resulting from several realistic hydrogen release scenarios are analyzed in chapter 3.1. On this basis, potential positions for recombiners are selected and the mitigated scenarios are assessed to identify the increased safety margins (chapter 3.2). Concluding, a summary and outlook are given in chapter 4.

2 MODELING APPROACH

2.1 Geometric Model

The engine room is located in the rear part of the hydrogen carrier, shown in Figure 2. Outside, at the rear side of the engine room (left in the picture), there is a gas hood. From the gas hood, hydrogen enters the engine room through pipes at the upper deck. There are three pipes which lead to the right main boiler and another three pipes which lead to the left main boiler. In both cases, the three pipes are housed in a rectangular, non-pressure-resistant protection tube. The hydrogen is transported through these pipes to the two main boilers which extend from the 2nd deck to the A-deck. The main boiler and the gas hood are sketched in red in Figure 2.

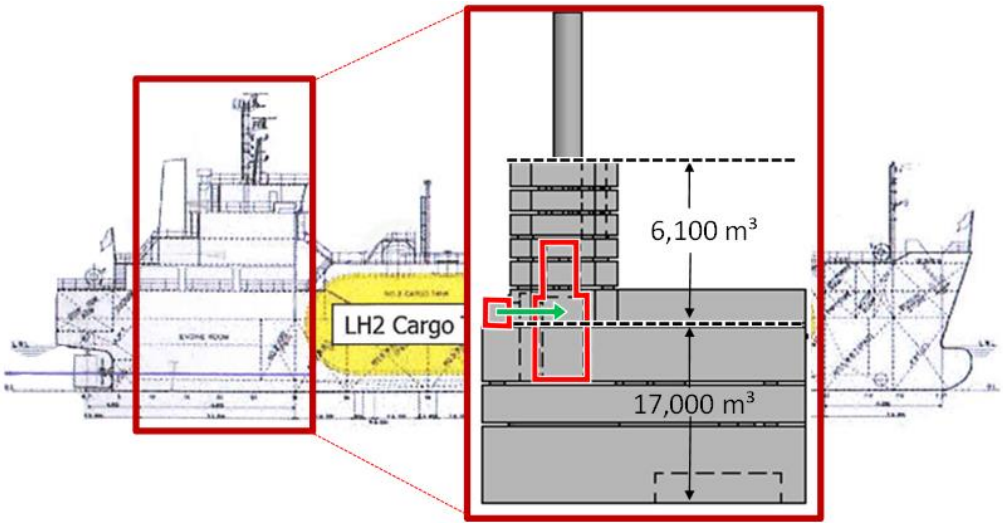

Figure 2. Spatial orientation of the engine room

In total, the engine room consists of eight decks and a funnel, shown in Figure 3.

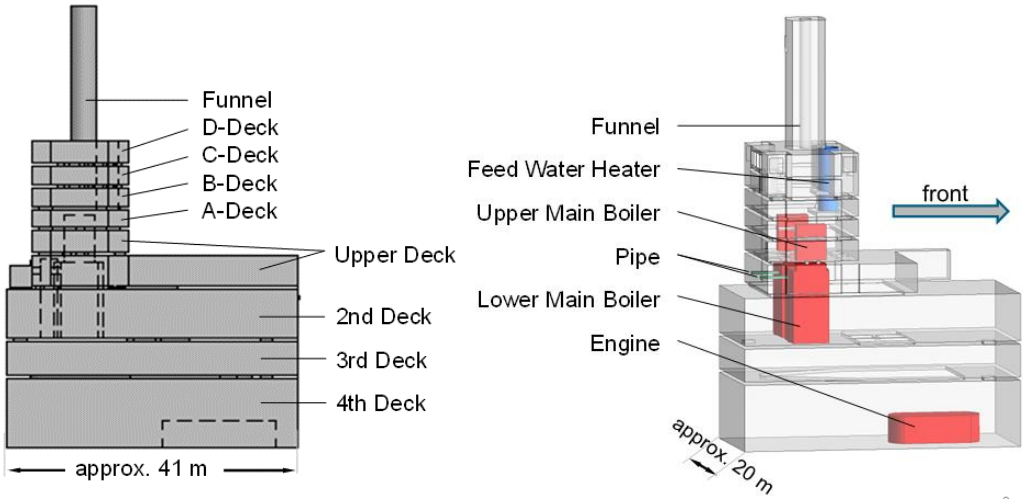

Figure 3. Designation of the different decks (left) and mapped installations (right)

From top to bottom, there are the D- to A-decks, the upper deck, and the 2nd to the 4th decks. While all decks are separated by ceilings, openings inside the ceilings connect the single fluid volumes as depicted in Figure 4.

From bottom to top, the lower ceiling of the 3rd deck has only one large opening of roughly 50 %. The bottom of the main boiler is located at the lower ceiling of the 2nd deck. This ceiling has several small openings which are mainly located at the center of the ceiling. In total, the opening area is approximately 50 % of the ceiling area. The ceiling between the 2nd deck and the upper deck is almost completely open, except for a small gallery around the side walls. The ceiling of the upper deck has 15 small openings, which open only 15 % of the ceiling area close to the walls, while the inner part of the ceiling is entirely closed. This ceiling is of particular importance as it is the ceiling above the expected hydrogen release. Hence the formation of a hydrogen-rich layer is expected under the ceiling of the upper deck. The flow through the opening will further govern the distribution of hydrogen. The ceilings of the bottom part of the A-deck and the upper decks primarily consist of small galleries and wide-open areas of approximately 80 %.

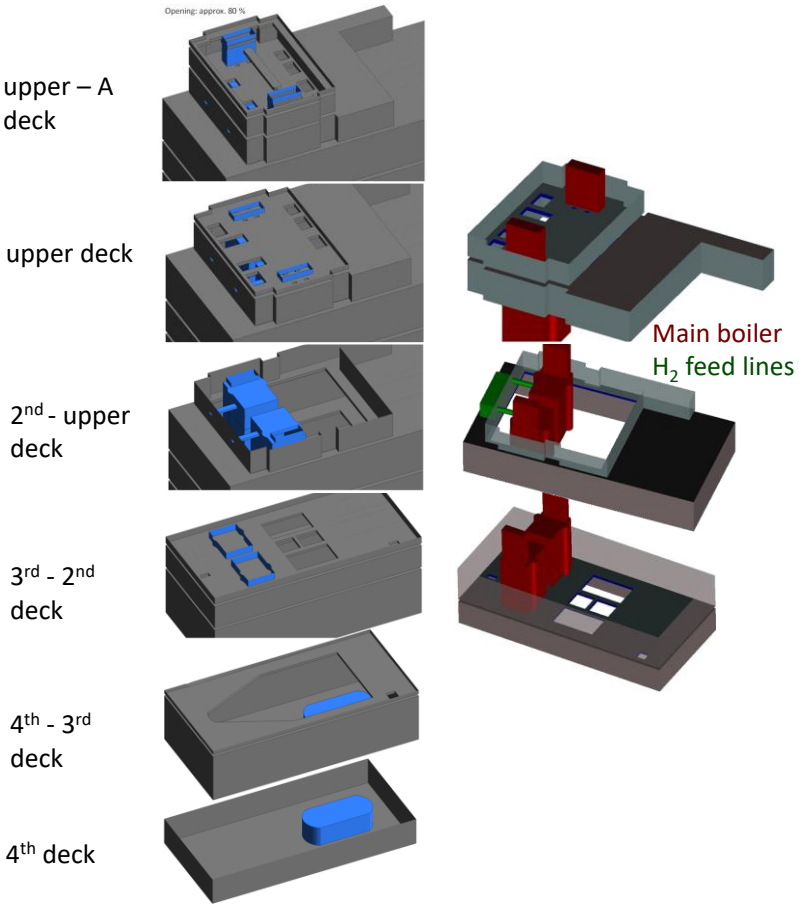

Figure 4. Ceilings between the decks (left) and main components (right)

On top of the D-deck, there is a 19 m high funnel which is in the current geometry connected to the engine room and the environment. The free gas volume of the decks above the hydrogen pipes including the deck with the hydrogen pipe amounts to 6,100 m³, the volume of the lower decks amounts to 17,000 m³. Beside the main boilers and the hydrogen feed lines, two further relevant major components are considered: The main engine, which represents a heat source in the lower decks that promotes buoyancy driven mixing, and the feed water heater, which is a large device that considerably reduces the free gas volume. The remaining equipment, piping and other components are not resolved in the model.

There are six connections between the engine room and the outside environment at different positions. One vent is located at the upper part at the funnel. This vent directly connects the engine room with the outside environment. As a protection against environmental influences, the vent is protected with exhaust louvers. These exhaust louvers are fix, there is always the possibility of gas exchange between the environment and the room of the propulsion system even if the blowers were not operating. The remaining five vents are located at the D-deck. Four vents are located in each of the corners of the deck. The fifth vent is located in the center at the back part of the engine room. Each of these vents is housed in a separate ventilation trunk. Blowers circulate air through these ventilation trunks to several positions and levels inside the engine room, while the ship is in normal operation. Between the entry of the ventilation trunks and the environment, there are exhaust fan louvers.

3.2 Placement of the PAR System

As discussed later in more detail, the simulation of an unmitigated hydrogen release scenario revealed four regions of potential hydrogen accumulation, where the installation of 10 recombiners might enhance the safety margins. The first reference concept (PAR-1) includes eight large (cross-section A~0.5m²) and two small recombiners (cross-section A~0.15m²). inside the engine room, see Figure 5.

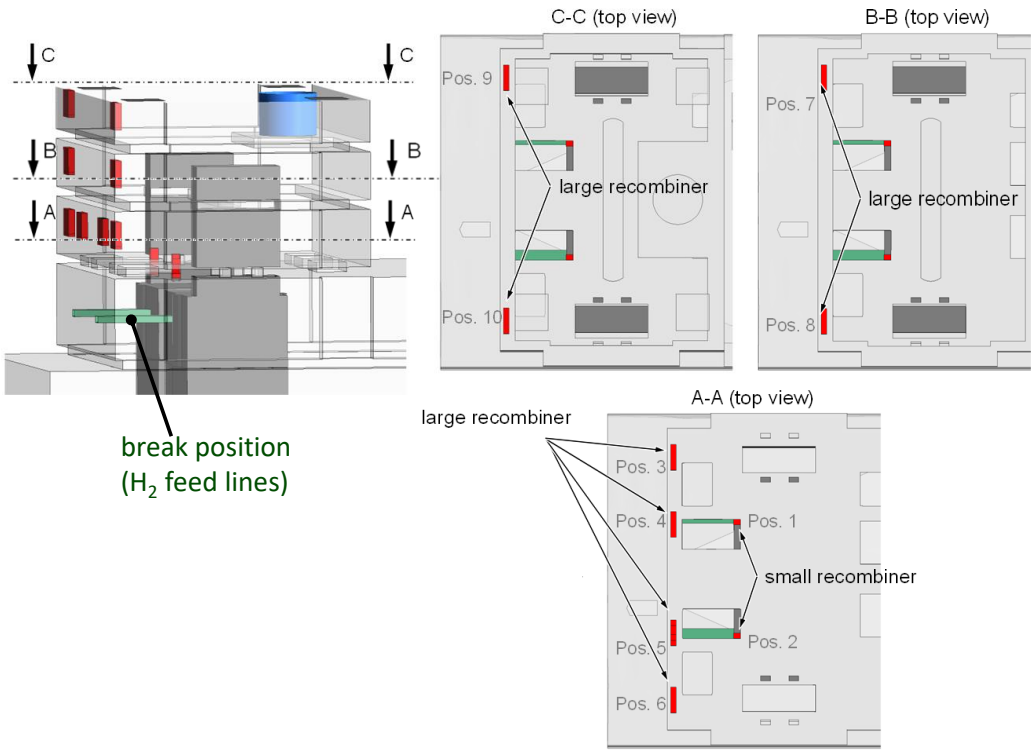

Figure 5. Placement of the PAR system – concept PAR-1.

The recombiners at the lowest position (position 1 and 2) are small recombiner units. They are placed inside the opening of the ceiling between the upper decks, which represents the dominant flow path of the hydrogen-rich plume. The inlet of the PARs is placed below the ceiling such that they can deplete hydrogen accumulated below the ceiling above the release location. The remaining 8 recombiners (position 3 to 10) are large recombiners. They are all located close to the back wall at different levels where a further hydrogen accumulation is observed due to flow stagnation in these regions. Four recombiners are placed at the upper deck which is closest to the hydrogen release, while the B and C decks are equipped each only with two PAR units.

Besides the basic concept PAR-1, the capacity (size) of the recombiner units is varied in two further analyses (PAR-2 and PAR-3 concepts) as summarized in Table 1.

Table 1. Variation of the recombiner types for the recombiners simulations.

Recombiner simulation	PAR type at positions 1 and 2	PAR type at positions 3 to 10
PAR-1	Small	Large
PAR-2	Large	Large
PAR-3	Large	Small

The comparative evaluation of the different PAR concepts serves as a basis to further analyze the required conversion capacity and enable a future optimization of the system.

3.3 Simulation Grid

The free volume is meshed with a fully hexahedral block-structured grid, using ANSYS ICEMCFD to obtain a mesh with high quality elements and limit the total number of required cells. Preliminary simulations of a hydrogen release revealed that nearly no hydrogen is transported to the decks below

the hydrogen release location. For that reason, the mesh resolution from the 4th deck to the 2nd deck is coarsened by a factor of 2 compared to the mesh resolution above the upper deck (see Figure 6), while the high mesh resolution in the upper decks ensures well resolved representation of the hydrogen transport. To resolve the flow induced by the PAR units, the mesh is locally further refined, as shown in Figure 7.

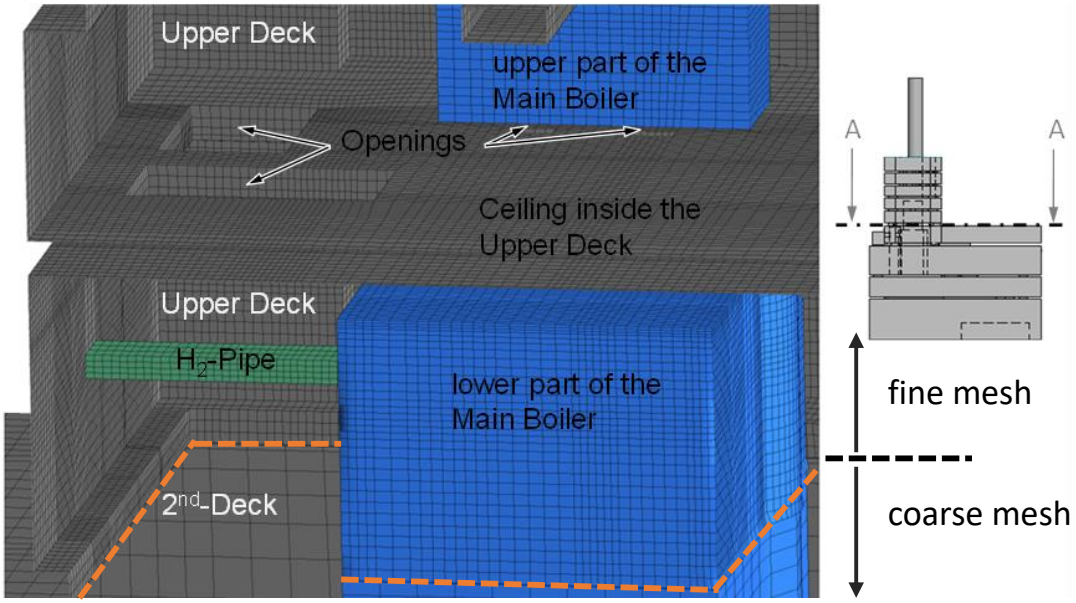

Figure 6. Visualization of the CFD grid with focus on the upper and 2nd decks.

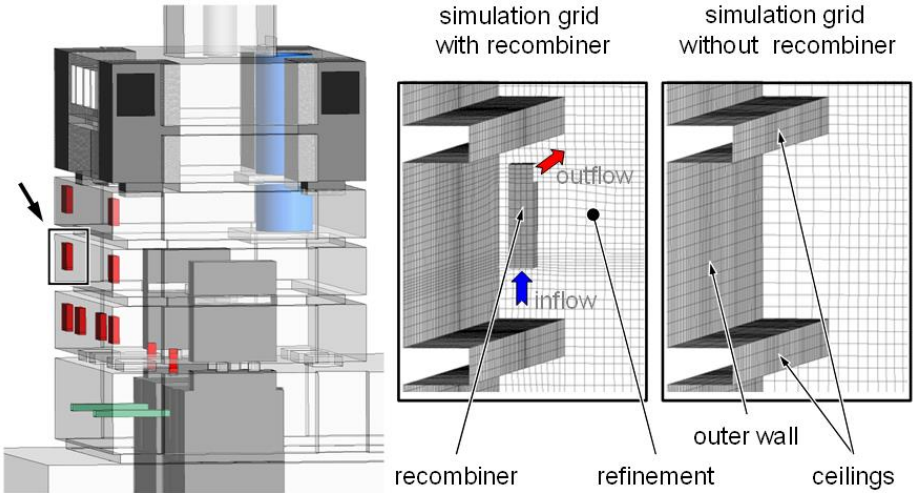

Figure 7. Visualization of the mesh refinement in the vicinity of the recombiners.

This refinement leads to an increase of the global mesh size by almost a factor of two compared to the grid for the unmitigated case, while the mesh quality is maintained at a consistently high level as summarized in Table 2.

Table 2. Grid statistics of the hexahedral mesh.

Mesh statistics	*without recombiners*	*with recombiners*
Total number of fluid elements	~ 1,600,000	~ 2,800,000
Volume size of an average volume (m^3)	~ 0.013	~ 0.008
Edge length of an average volume (m)	~ 0.24	~ 0.20
Grid Quality Metrics		
Aspect ratio	< 9	< 9
Cell volume ratio / growth rate	< 6.0	< 6.0
Minimum face angle (°)	> 27	> 27

During mesh generation, the established best practice guidelines [8,9] have been followed to minimize discretization errors. Nonetheless, a formal mesh sensitivity study was not yet conducted within the initial state of the study, but will be considered for future work.

2.4 Modeling of the Hydrogen Mixing and Transport Processes

The baseline model developed at Forschungszentrum Jülich for the analysis of hydrogen mixing and mitigation is employed [10]. For the sake of brevity, only the most relevant characteristics of the physical model and numerical settings are summarized in Table 3. Only the gas volume is modeled. Condensation and thermal radiation heat transfer is neglected due to low temperature differences and humidity. The fluid consists of a variable, ideal mixture of ideal gases. The unsteady Reynolds averaged Navier-Stokes (U-RANS) equations are closed by the k-ω-SST turbulence model which is the de facto standard for industrial applications [11].

The numerical settings are chosen to enable a 2^{nd} order accurate solution and sufficient transient resolution. The convergence criterion offers a good compromise between a highly accurate solution and calculation time.

Table 3. Baseline model for hydrogen mixing and mitigation [10].

Governing Equations	U-RANS equations, thermal energy equation, species equation for O_2, H_2 and H_2O (N_2 is constraint component)
Turbulence	SST turbulence model incl. buoyancy turbulence production & dissipation terms based on the Simple Gradient Diffusion Hypothesis (SGDH) model
Equation of State	ideal gas equation of state
Material properties	constant transport properties according to [10]
Numerical schemes	high resolution advection scheme, 2^{nd} order Euler-backward
Time steps	adaptive: ave. Courant Number = 1 (Δt = ~ 0.3 s)
Convergence criteria	max. residual < 1E-3 (~ RMS < 1E-5), min. 3 PIMPLE iterations

2.5 Boundary and Initial Conditions

The considered thermal initial and boundary conditions are representative for a typical ocean cruise and summarized in Figure 8. Nevertheless, it should be stressed that they can vary significantly depending on the weather conditions.

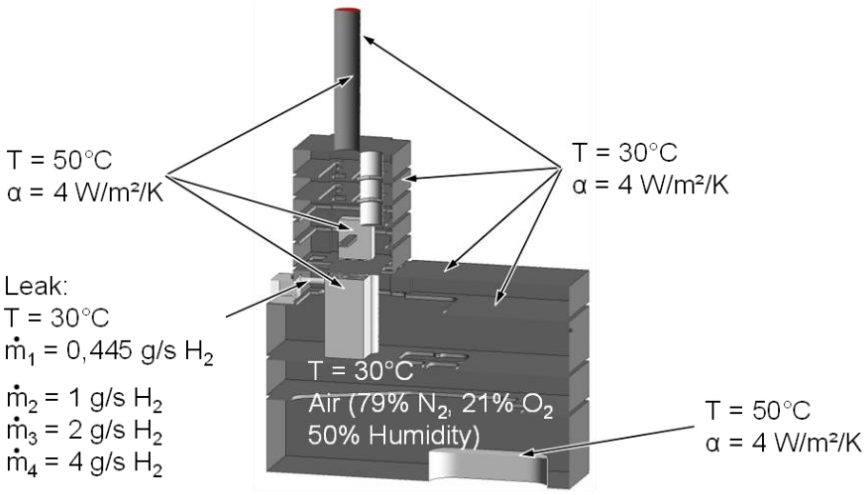

Figure 8. Boundary and initial conditions.

The ventilation ducts are protected against environmental impact by means of exhaust louvers with fixed fins. Thus, they represent permanently open boundary conditions in the CFD model which enable both inflow and outflow. The outside environment is defined as humid air of 50 % relative humidity and 30 °C. The pressure loss coefficient of the exhaust louvers is estimated with ξ=6.5 based on Idelchik [12]. Under normal operation, a blower drives the air through the ventilation system. In case of the considered power blackout, the blower, however, represents an additional flow resistance which is estimated by an additional pressure loss coefficient of ξ=15 [12].

Hydrogen is injected at a constant rate assuming an undetected leak at the left hydrogen pipe, close to the main boiler. Four release scenarios with rates from ~0.5 g/s up to 4 g/s are considered, which were estimated based on the model by Saint-Venant and Wantzel [13]. Preliminary simulations revealed that the momentum and the direction of the leaking hydrogen do not influence the resulting global flow patterns due to the strong buoyancy effects.

3 RESULTS

3.1 Unmitigated Scenario

The released hydrogen instantly forms a buoyant plume due to the large density difference between the hydrogen and the ambient air. When passing through the ceilings the hydrogen plume breaks up, which promotes mixing. Consequently, hydrogen disperses almost homogeneously throughout the upper decks above the injection elevation and the hydrogen concentration decreases rapidly from 100 vol.% at the release position down to few percent. The lighter hydrogen-air mixture rises to the top of the engine room where the hydrogen/air mixture leaves the engine room through the vents. At the same flow rate, pure air enters the engine room through the other vents at deck D. This heavier air falls to the lower part of the engine room so that a natural circulation is formed, which removes a considerable part of the released hydrogen from the engine room to the environment. Consequently, the present hydrogen mass inside the engine room is considerably less than the integrally released hydrogen mass (Figure 9). Generally, it can be concluded that higher release rates result in a higher hydrogen mass inside the machine room. However, the resulting strong density differences between machine room and ambient air promote the natural circulation venting (~1 m³/s) and counteract the hydrogen accumulation to a certain extent. It must be stressed that the natural circulation depends also

on the internal flow resistances (e.g. piping, components, walking grids etc.) which are not resolved in the simulation.

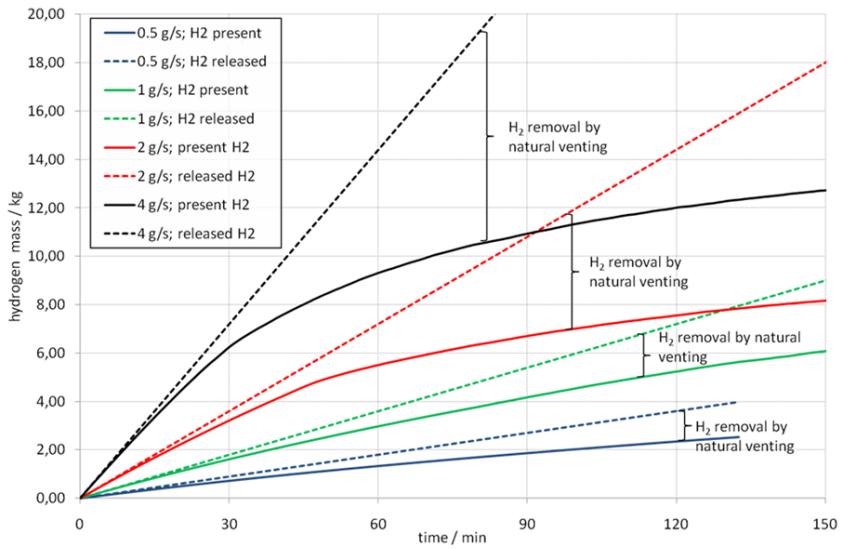

Figure 9. Comparison between the released mass of hydrogen and the actual mass of hydrogen.

The accumulation of hydrogen inside the machine room leads to a formation of hydrogen-rich clouds depending on the release rate. Figure 10 illustrates the hydrogen distribution for a rate of 4g/s at two time points.

Generally, it can be concluded that a hydrogen release at rates of 0.5 and 1 g/s does not result in a considerable flammable gas cloud determined at lower flammability limit of 4 vol.%. However, for higher release rates, flammable clouds of ~8 m³ (2 g/s) and ~30 m³ at a release rate of 4 g/s hydrogen occur as a ceiling layer within the first 90 min after pipe break. Inside this layer, the concentrations are higher than 4 vol.%, while above the ceiling, the hydrogen concentration decreases rapidly due to the mixing downstream the openings. In the upper engine room, there are mainly two distinct regions with a hydrogen concentration above 2 vol.%: First, the hydrogen-rich plumes above openings inside the ceiling; second, a hydrogen accumulation close to the wall at the rear side of the engine room where flow is stagnating.

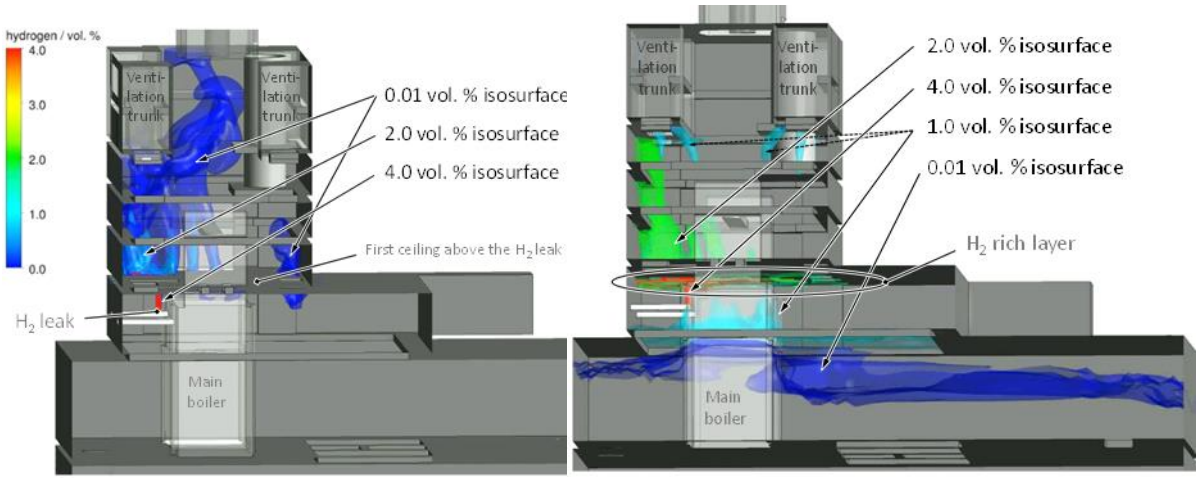

Figure 10. Visualization of the hydrogen concentration by isosurfaces at 10 min (left) and 90 min (right) after the release – 4 g/s scenario.

It should be recalled that these results were obtained for a single set of boundary conditions and depending on the ambient air temperature, humidity, and wind conditions the natural venting rate and thus the overall hydrogen accumulation may differ in both directions. Nonetheless, it can be concluded that the location of the hydrogen-rich clouds is above the injection lines and the PAR units should be placed here (as illustrated in chapter 3.2).

3.2 Mitigated Scenarios

The amount of hydrogen which can be removed by the recombiners depends strongly on the position of the recombiners and on the size/capacity of the recombiners. In case of the engine room, the recombiner positions are chosen to prevent hydrogen accumulations, while globally the hydrogen mass inside the compartments is limited by the natural circulation venting. In the following, the reference PAR system PAR-1 (compare chapter 3.2) is discussed in detail and results for the other concepts PAR-2 and PAR-3 are compared. Figure 11 gives a general impression of the effect of recombiners operation on the hydrogen accumulation zones.

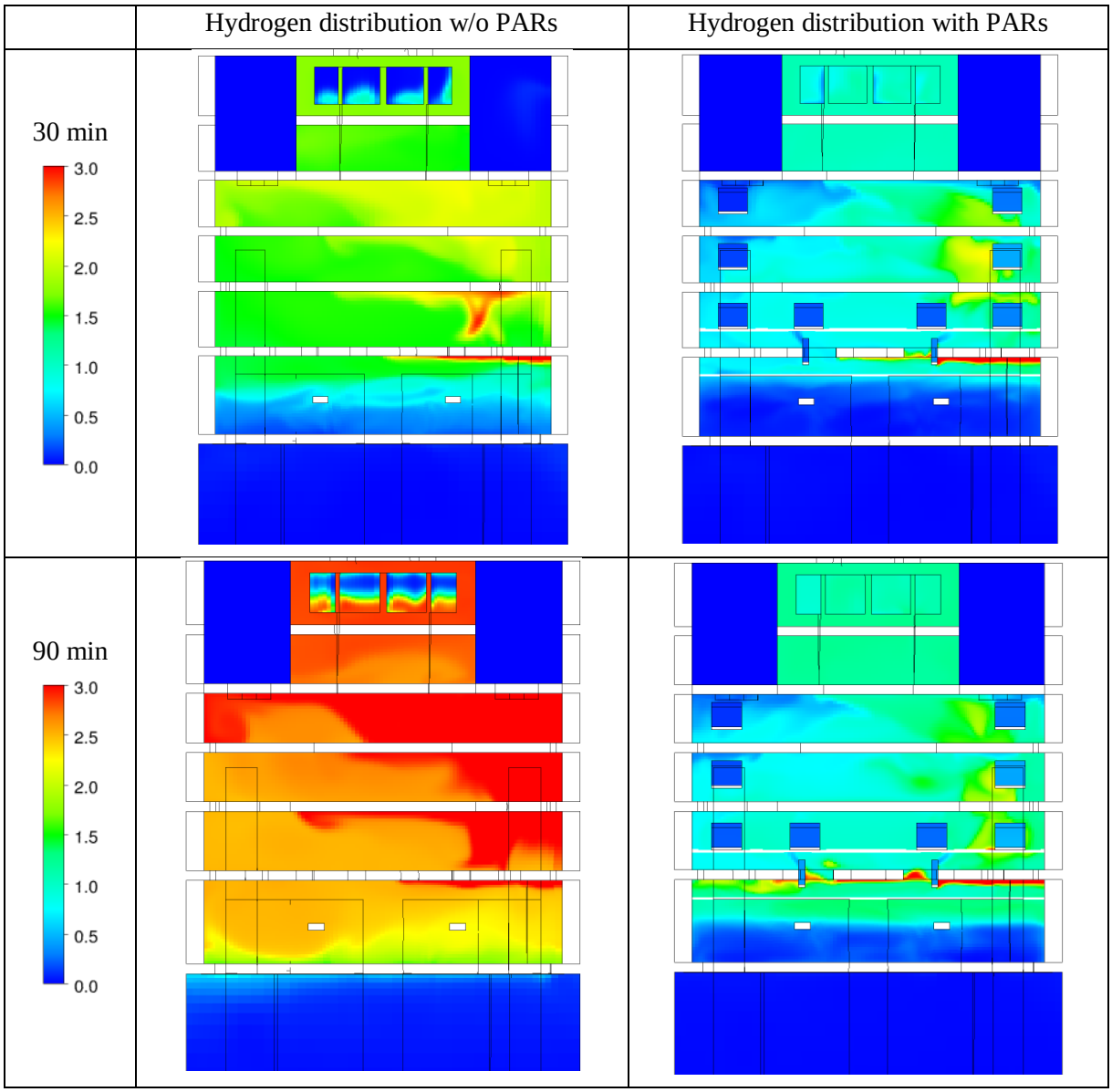

Figure 11. Hydrogen accumulation at a 2D plane through the stagnation region close to rear wall with (right) and without PAR installation (left).

The color bar representing the hydrogen concentration is limited to 3 vol.% to promote comparison. During the scenario, hydrogen accumulates inside the shown stagnation area especially next to the hydrogen release position. The same view to the scenario with recombiners shows hydrogen concentrations which are significantly lower. The reduction has two reasons. First, there is a hydrogen reduction by the recombiners itself. Second, there is the stronger effect of inducing a flow through this stagnation area by the hot recombiner exhaust gas plume, which further promotes mixing and natural circulation. As a result, the amount of hydrogen is significantly reduced by the recombiners as shown in Figure 12.

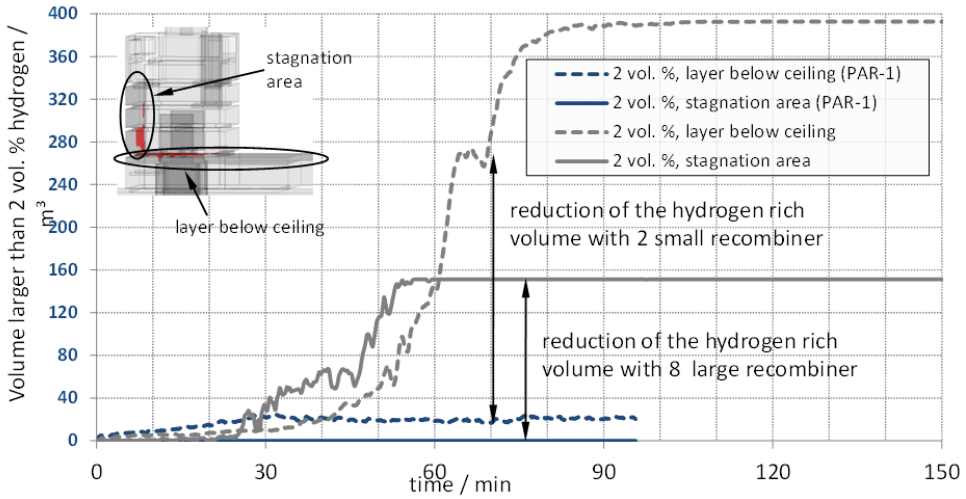

Figure 12. Effect of the PARs on the 2 vol. % cloud inside the stagnation area and the layer below the ceiling.

In both regions, there is a strong reduction of the hydrogen accumulation (here illustrated by the volumes containing > 2 vol.%) by the recombiner system. Consequently, the safety margins are significantly enhanced. To assess the impact of the PAR capacity, the three different PAR arrangements (see Table 1) are compared for the 4 g/s release scenario. All three PAR concepts reduce the mass of hydrogen visibly as shown in Figure 13. A first indication about the effect of the PAR size (i.e. conversion capacity) can be obtained by comparing the curve of concept PAR-3 (2 large, 8 small PAR units) against concept PAR-2 (10 large PAR units). The conversion rate of the reference concept PAR-1 (2 small, 8 larger PAR units) is close to the one of concept PAR-2.

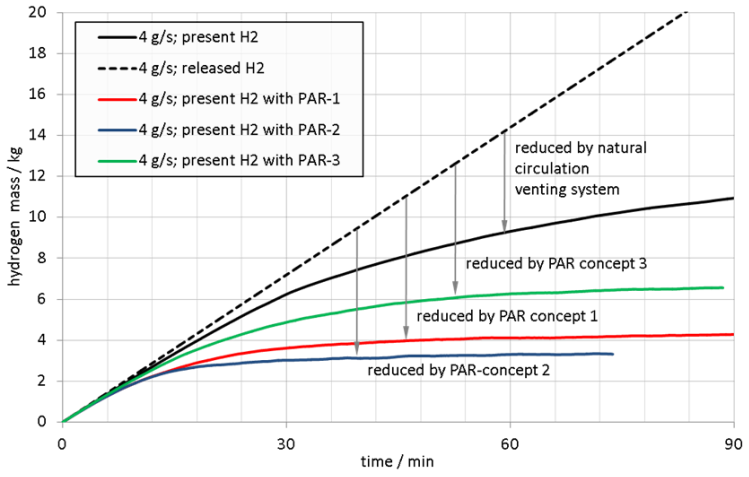

Figure 13. Integrated hydrogen mass in the engine room for different PAR concepts.

The effect of the PAR size can be assessed by comparing the integrated conversion rates at the same position for a large (concept PAR-2) and a small PAR unit (concept PAR-3). It must be stressed that this is a qualitative result, due to the fact that the conversion rate is determined by the available hydrogen which is different in both simulations. Figure 14 compares the transient integrated recombined mass at t=60 min after break, when a nearly steady hydrogen mass in the engine room is reached (see Figure 13). While a larger PAR recombines generally more hydrogen, one can identify that the recombination rate does not linearly scale with the PAR size.

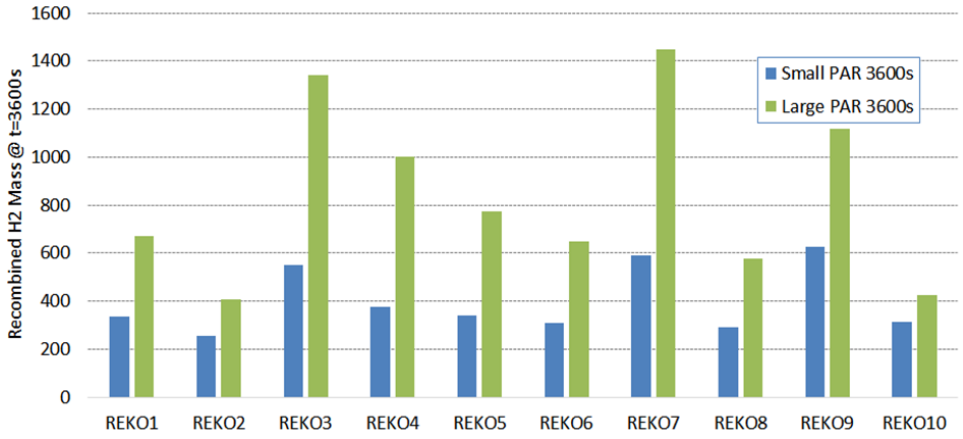

Figure 14. Comparison of the integrated conversion rates at t=60 min for different PAR unit sizes at different positions.

Both PAR units REKO1 and REKO2 mounted in the flow path of the hydrogen plume show a comparably low conversion rate, however, significantly contribute to the reduction of hydrogen concentrations and thus the overall risk. Concluding, in the considered scenario, the capacity of a large PAR unit is not fully exploited. Consequently, the use of an increased and more evenly distributed number of small PAR units may be more efficient in terms of hydrogen removal and mixing. Furthermore, the positioning of a small PAR unit is easier to realize and more flexible compared to a large one.

4 CONCLUSIONS

Hydrogen leaking from the feed lines into the engine room is considered in the frame of risk analyses for future LH2 carriers. The hydrogen distribution inside the engine room has been simulated for different release scenarios including hydrogen release rates between 0.5 – 4.0 g/s. Based on these scenarios, the efficiency of three different PAR arrangements has been investigated. The CFD simulation of the hydrogen distribution for different hydrogen release scenarios reveals that the special geometry of the engine room with the venting position promotes a natural circulation venting effect. This natural circulation venting effect reduces the amount of hydrogen and promotes a homogeneous hydrogen distribution inside the upper part of the engine room. However, two regions are identified where hydrogen accumulation occurs: A hydrogen rich layer below the first ceiling above the hydrogen supply pipes and a stagnation region at the back side of the ship. In both regions, significant gas volumes with hydrogen concentrations > 2 vol.% are present.

Consequently, the prototypic implementation of 10 PAR units in these regions was further investigated. The simulations were performed with three different PAR arrangements of large and small PAR units. For the investigated geometry (engine room, leak position, PAR position, etc.) it can be confirmed that the PARs reduce efficiently the hydrogen accumulation in terms of mass and volume of the hydrogen-rich cloud. The efficiency of a PAR unit is related to the converted hydrogen mass but also to the induced mixing processes and thus the dilution of the hydrogen-rich clouds. However, the impact on the mixing process is hard to quantify. Considering the converted hydrogen mass, the contribution of the PARs differs. For a further optimization of the PAR system, also the

reduction in concentration (PAR outlet vs. PAR inlet) needs to be considered as this provides a dominant contribution to risk reduction. Comparing the performance of a small and large PAR unit at the different positions, it becomes obvious that the full capacity of a large PAR unit is not completely exploited. Consequently, the installation of an increased number of more evenly distributed small PAR units is rated more efficient in terms of hydrogen depletion and mixing. Furthermore, the reduced space requirements of small PAR units allow for a more flexible positioning inside the engine room.

Considering in particular the impact of different ambient boundary conditions on the natural circulation venting could support generalizing the conclusions.

REFERENCES

1. Nishimura, M., Shindo, K., Yoshimura, K. and Yoshino, Y., Activities for Realization of International Liquefied Hydrogen Energy Supply Chain, Kawasaki Technical Review, No. 182, 2021.
2. Muragishi, O., Inatus, S., Uraguchi, R., Yamashiro, K., Imai, T., Ohashi, T., Shimogaki, T., Yoshida, T., Koumoto. T., Hydrogen Transportation - Development of Liquefied Hydrogen Carrier, Kawasaki Technical Review, No. 182, 2021.
3. Liang, Z., Sonnenkalb, M., Bentaib, A. and Sangiorgi, M., Status Report on Hydrogen Management and Related Computer Codes, OECD/NEA Report, NEA/CSNI/R(2014)8.
4. Areva GmbH, Passive Autocatalytic Recombiner, Product information, 2013.
5. ANSYS Inc., CFX Solver Theory Guide, Release 15, 2013.
6. Jaekel, Ch., Kelm, S., Reinecke, E.-A., Verfondern, K. and Allelein, H.-J., Validation strategy for CFD models describing safety-relevant scenarios including LH2/GH2 release and the use of passive auto-catalytic recombiners, *International Journal of Hydrogen Energy*, **39**, 2014, pp. 20371-20377.
7. Reinecke., E.-A., Kelm, S., Steffen, P.-M., Klauck, M. and Allelein, H.-J., Validation and Application of the REKO-DIREKT Code for the Simulation of Passive Autocatalytic Recombiner Operational Behavior, *Nuclear Technology*, **196**:2, 2016, pp. 355-366.
8. Mahaffy, J. et. al., Best Practice Guidelines for the Use of CFD in Nuclear Reactor Safety Applications – Revision, OECD/NEA Report, NEA/CSNI/R(2014)11.
9. ERCOFTAC, Industrial Computational Fluid Dynamics of Single-phase Flows ERCOFTAC Best Practice Guidelines, 2013.
10. Kelm, S., Müller, H. and Allelein, H.-J., A Review of the CFD Modeling Progress Triggered by ISP-47 on Containment Thermal Hydraulics, *Nuclear Science and Engineering*, **193**1-2, 2019, pp. 63-80.
11. Menter, F., Kuntz, M. and Langtry, R., Ten Years of Industrial Experience with the SST Turbulence Model, *Heat and Mass Transfer* **4**, 2003.
12. Idelchik, I.E., Handbook of Hydraulic Resistance, 3rd Edition, Moscow, 2005.
13. Verein Deutscher Ingenieure(VDI), Waermeatlas, Springer, 10th ed., 2006.